# Synergistic Laser-Wakefield and Direct-Laser Acceleration in the Plasma-Bubble Regime

Xi Zhang, Vladimir N. Khudik, and Gennady Shvets
*Department of Physics and Institute for Fusion Studies, The University of Texas at Austin, Austin, Texas 78712, USA*
(Received 19 December 2014; published 6 May 2015)

The concept of a hybrid laser plasma accelerator is proposed. Relativistic electrons undergoing resonant betatron oscillations inside the plasma bubble created by a laser pulse are accelerated by gaining energy directly from the laser pulse and from its plasma wake. The resulting phase space of self-injected plasma electrons is split into two, containing a subpopulation that experiences wakefield acceleration beyond the standard dephasing limit because of the multidimensional nature of its motion that reduces the phase slippage between the electrons and the wake.

DOI: 10.1103/PhysRevLett.114.184801 PACS numbers: 41.75.Jv, 52.35.Mw, 52.38.Kd

Advances in laser technology are transforming the idea of laser-based acceleration of charged particles into one of the most promising high-gradient concepts [1]. Broadly speaking, laser acceleration concepts can be divided into two classes: far-field particle accelerators, where acceleration is accomplished by transverse laser fields that do not require any external electromagnetic structures, and near-field particle accelerators, where the laser field is significantly modified by the presence of a linear or nonlinear medium. In a typical far-field accelerator, such as an inverse free-electron laser [2,3] or inverse ion-channel laser [4–6], relativistic electrons executing undulating or betatron motion gain energy directly from the laser. On the contrary, in the near-field laser-wakefield acceleration (LWFA) [7] regime, the electrons gain energy indirectly from the electric field of the plasma wave that is excited by a laser pulse.

Several unique features of plasmas conspire to make LWFA one of the most exciting near-field acceleration concepts of the past decade [8–10]: the high accelerating gradient, the available pool of electrons supplied by the plasma acting as an injector, and the replaceability of the plasma accelerating structure after each laser pulse. The strongly nonlinear regime of LWFA, corresponding to the complete blow out of the plasma electrons from the laser's path [11,12], is particularly promising for generating high-energy monoenergetic electron beams [13–15] that have recently reached GeV-scale energies [16–18]. The key enabling mechanism for narrow energy spread is the electron injection into the resulting plasma "bubble" over a short distance accomplished by engineering either the plasma density ramp [19–23] or the rapid variation of the bubble's size during self-focusing [17,24] along the laser's path. However, phase slippage (dephasing) between the electric field inside the bubble propagating with subrelativistic speed $v_b$ and ultrarelativistic electrons comoving with the bubble with $v_x \approx c$ limits the energy gain. Energy spread can also be reduced through phase space rotation [25] or beam loading [26].

Far-field plasma-based direct-laser acceleration (DLA) has also been considered in the past [4,27–31], especially in the context of developing efficient x-ray and $\gamma$-ray radiation sources [27,32–34]. DLA occurs when the laser pulse transfers energy and momentum to relativistic electrons undergoing betatron oscillation in a partially [5,28,29] or fully [27,32–34] evacuated plasma channel. For a laser pulse with frequency $\omega_L$ and phase velocity $v_{\rm ph}$ to resonantly interact with a copropagating electron executing betatron motion with frequency $\omega_\beta$, the following resonance condition must be satisfied over the length of the plasma: $\omega_d \equiv \omega_L(1 - v_x/v_{\rm ph}) = \pm\omega_\beta$. The main limitation of DLA is that, generally, the experimentally measured energy distribution of the accelerated electrons is Boltzmann-like [4,5]. Considerable improvement in laser-plasma acceleration could be achieved if energy gains from the laser and from the wakefield were combined while maintaining (or even reducing) the narrow energy spread characteristic of self-injected bubble-regime LWFAs [17].

It is by no means obvious that such a synergistic combination of the two acceleration mechanisms is possible. For example, rapid particle acceleration by the plasma wakefield can rapidly detune the betatron resonance, as well as damp the amplitude of the betatron motion [27] that determines DLA's accelerating gradient [4]. The laser pulse profile that is optimal for DLA may affect the structure of the plasma bubble, thereby reducing the energy gain from the wake and/or inhibiting self-injection. In this Letter we demonstrate that the two mechanisms can, in fact, act synergistically, with DLA significantly increasing the LWFA energy gain by extending the dephasing length. Using particle-in-cell (PIC) simulations, we predict the emergence of two distinct groups of self-injected electrons separated in time and in phase space: the high-energy DLA group that experiences large energy gains from both acceleration mechanisms, and the lower-energy non-DLA group that experiences no energy gain from the DLA mechanism, and smaller energy gain from the LWFA mechanism. The larger LWFA experienced by the DLA

 

population relative to the non-DLA group is shown to be caused by the former experiencing delayed dephasing from the wake.

Before presenting the results of self-consistent PIC simulations that model all aspects of the laser evolution, electron injection, acceleration, and separation into DLA and non-DLA populations, we first develop a qualitative understanding of hybrid DLA and LWFA using test-particle simulations of electron dynamics in the combined wake-field and laser fields. We adopt a simplified description [27,33,34] of the electromagnetic fields in the 2D ($x$-$z$) geometry. The accelerating and focusing wakes inside a spherical bubble with radius $r_b$ propagating with relativistic velocity $v_b \approx c(1-1/2\gamma_b^2)$ are approximated as $W_x = m\omega_p^2(x-r_b-v_b t)/2e$ and $W_z = m\omega_p^2 z/2e$, respectively, where $\omega_p = \sqrt{4\pi e^2 n/m_e}$ is the plasma frequency, $n$ is the plasma density, and $m_e$ is the electron mass. Note that (a) the wake fields are the combinations of the electric and magnetic forces [38], and (b) the accelerating wake changes sign at the bubble's center $\zeta \equiv x - v_b t = r_b$.

For simplicity, the linearly polarized laser fields were assumed to be planar and given by $E_z^{(L)} = -E_0 \sin\omega_L(t-x/v_{\rm ph})$ and $B_y^{(L)} = B_0 \sin\omega_L(t-x/v_{\rm ph})$, where $B_0 = cE_0/v_{\rm ph}$. The equations of electron motion are then given by

$$\frac{dp_x}{dt} = -e\left(W_x - \frac{v_z}{c}B_y^{(L)}\right),$$
$$\frac{dp_z}{dt} = -e\left(W_z + E_z^{(L)} + \frac{v_x}{c}B_y^{(L)}\right), \quad (1)$$

and the following laser and plasma parameters scaled to the laser wavelength $\lambda_L = 2\pi c/\omega_L = 0.8\ \mu$m were chosen for the simulations below: $\omega_p/\omega_L = 0.032$ (corresponding to plasma density $n = 1.8\times10^{18}$ cm$^{-3}$), $r_b = 22\lambda_L$, $\gamma_b = 18$, and $E_0 \approx 2.5 m_e c\omega_L/e$. For these parameters the peak accelerating gradient $E_{\rm max}^{(W)}$ at the back of the bubble ($x = v_b t$) is $E_{\rm max}^{(W)} \approx E_0/40 \approx 2$ GV/cm. These parameters were chosen to approximately mimic the parameters of PIC simulations presented below. From Eq. (1), the natural betatron frequency of an electron with relativistic factor $\gamma$ is $\omega_\beta = \omega_p/\sqrt{2\gamma}$.

We first consider the case of a subluminal laser pulse with $v_{\rm ph} = 0.9985c$ [27]. Although the proposed approaches to achieving $v_{\rm ph} < c$ such as using cluster plasmas [35], residual non-neutral gas [36], or corrugated plasma waveguides [37] are challenging to implement in the context of ultraintense laser pulses, we briefly analyze the subluminal case below because it provides a stark illustration of the delayed dephasing via direct laser-electron interaction. Test electrons are injected at $t = 0$ near the back of the bubble at $x = 2.65\lambda_L$ with a constant value of $\gamma = 25$. The initial transverse positions $z$ and momenta $p_z$ were chosen to span a

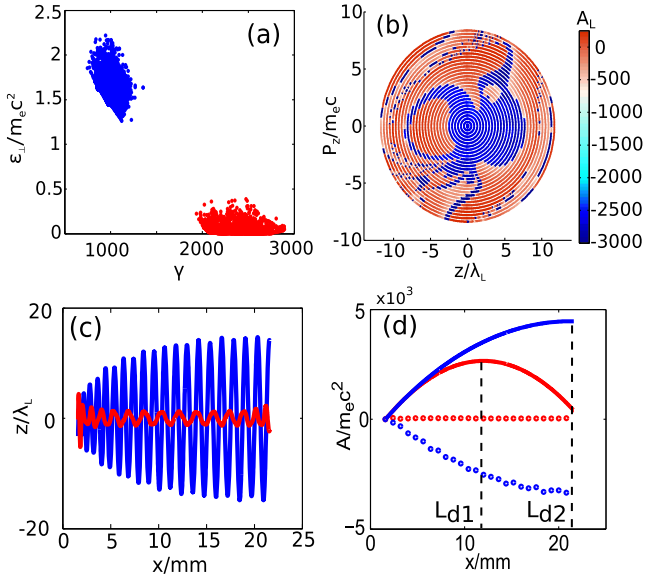


FIG. 1 (color online). Single-particle dynamics in combined wake and laser fields with $v_{\rm ph} < c$. (a) Fragmentation of the $(\gamma, \epsilon_\perp)$ phase into DLD (blue) and non-DLD (red) electron populations at $x = 1.3$ cm. (b) Color-coded laser energy gain $A_L$ as a function of the initial conditions in the $(z_0, p_{z0})$ phase space. Elliptical curves: $\epsilon_\perp = $ const. (c) Betatron trajectories of two representative electrons from the DLD (blue line) and non-DLD (red line) groups. (d) Energy gain by the same representative electrons from the wake ($A_W$, solid lines) and from the laser ($A_L$, dashed lines).

wide range $0 < \epsilon_{\perp 0}/m_e c^2 < 1$ of transverse energies [38,39] $\epsilon_\perp = p_z^2/2\gamma m_e + \gamma m_e \omega_\beta^2 z^2/2$.

The bifurcated $(\gamma, \epsilon_\perp/m_e c^2)$ phase space of the injected test electrons after the propagation distance of $x = ct = 1.3$ cm is shown in Fig. 1(a): one group of electrons (blue) gains considerable transverse energy $\epsilon_\perp$ from the laser while the other group (red) experiences considerable reduction in $\epsilon_\perp$. By following two representative electrons [one from each group, see Fig. 1(b) for the initial phase space color coded by the final energy gain, and Fig. 1(c) for the electrons' trajectories], the following properties of the two groups are observed. (i) *Direct laser deceleration (DLD)*: the work $A_L = -\int eE_z^{(L)} v_z dt$ done by the laser field on the first group of electrons (blue lines in Fig. 1) is negative as shown by the dashed line in Fig. 1(d). The non-DLD electrons do not exchange energy with the laser pulse. The physics of DLD is related to the anomalous Doppler effect (i.e., $-\omega_d = \omega_\beta$) that has been investigated in dielectric-loaded or periodically loaded waveguides [40,41]. Qualitatively, if an ultrarelativistic ($\gamma \approx p_x/m_e c \gg 1$) electron interacts with the laser alone, a simple relationship between the changes in $\epsilon_\perp$ and $\gamma$ can be derived: $\Delta\gamma(1 - c/v_{\rm ph}) = \Delta\epsilon_\perp/mc^2$, thus implying that DLD ($\Delta\gamma < 0$) is necessary for the resonant excitation of betatron oscillations ($\Delta\epsilon_\perp > 0$) whenever $v_{\rm ph} < c$. The above relation holds under the near-relativistic assumption for the laser pulse: $|1 - v_{\rm ph}/c| \ll 1$.

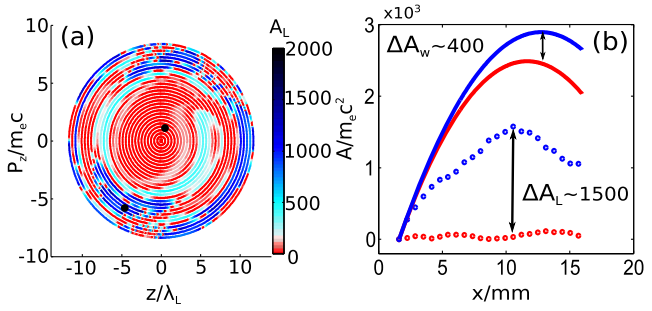


FIG. 2 (color online). Single-particle dynamics in combined wake and laser fields with $v_{\rm ph} > c$. (a) Same as in Fig. 1(b). (b) Energy gain from the laser or wake ($A_L$, dashed lines; $A_W$, solid lines) for two test electrons with initial conditions marked in (a) by the black dots. Blue lines: DLA. Red lines: non-DLA test electrons. All other parameters are the same as in Fig. 1.

(ii) *Laser-delayed dephasing* is apparent from Fig. 1(d) (solid lines), where the wake energy gain of the DLD electron persists much longer than that of the non-DLD electron: $L_{d2} \approx 2L_{d1}$. The dephasing rate $d\zeta/dt = v_x - v_b$ is suppressed by the resonant excitation of the betatron oscillation according to

$$\frac{d\zeta}{d(ct)} \approx \frac{1}{2\gamma_b^2} - \frac{1 + \langle p_z^2/m_e^2c^2\rangle}{2\gamma^2}, \qquad (2)$$

where $\langle p_z^2\rangle \approx \gamma m_e \epsilon_\perp$ represents the time-averaged betatron oscillation momentum. An important manifestation of the delayed dephasing for DLD electrons is that they experience much greater energy gain $A_W = -\int eW_x v_x dt$ from the wakefield compared with non-DLD electrons. Note, however, that the total energy gain $A = A_W + A_L$ is smaller for DLD electrons because they amplify the laser pulse at the expense of the energy gained from the wake.

Next, we consider a more realistic case of the superluminal phase velocity ($v_p = 1.00036c$ corresponding to laser propagation in a plasma with $n = 1.8 \times 10^{18}$ cm$^{-3}$; all other laser or wake parameters and initial conditions of the test electrons are the same as in the subluminal case). In the $v_{\rm ph} > c$ case the electrons gaining transverse energy are also gaining energy from the laser, i.e., $A_L > 0$. It is apparent from Fig. 2(a) that, while $A_L$ depends on the initial phase of the electron's betatron oscillation (i.e., on the specific values of $p_{z0}$ and $z_0$), a large initial value of the transverse energy is a precondition for DLA.

Laser and wake energy gains of two representative DLA (blue) and non-DLA (red) electrons with initial transverse energies $\epsilon_{\perp 0} = 0.8 m_e c^2$ and $\epsilon_{\perp 0} = 0.1 m_e c^2$, respectively, are compared in Fig. 2(b). The synergistic nature of the hybrid DLA and LWFA is apparent: the DLA electron gains more energy from the wake than a non-DLA electron, with the difference of $\Delta A_W \approx 0.2$ GeV being due to delayed dephasing. At the same time, the DLA electron gains $A_L \approx 0.7$ GeV energy from the laser, thereby almost doubling its total final energy $\epsilon_{\rm tot} \equiv \gamma m_e c^2$ compared with its non-DLA counterpart.

Based on the results of single-particle modeling, we can now formulate the conditions for achieving synergistic DLA and LWFA in a realistic laser-plasma accelerator. First, considerable overlap between the laser field and injected electrons is required for effective DLA. Second, electrons must be injected into the bubble with large transverse energy. We use a 2D PIC code VLPL [42] to model the self-consistent interaction of a multiterawatt laser pulse with tenuous ($n = 1.8 \times 10^{18}$ cm$^{-3}$) plasma to demonstrate that these two conditions can be met. The first condition is satisfied by employing two laser pulses [labeled as pump and DLA in Fig. 3(a); see the caption for laser or plasma and computational grid parameters], where a much weaker time-delayed DLA pulse has no observable effect on the bubble shape and accelerating field, yet enables DLA by overlapping with self-injected electrons.

The second condition is met by engineering the self-injection of the background plasma electrons into the bubble. A short injection density bump shown in Fig. 3(a) is utilized to rapidly deform the plasma bubble, thereby causing self-injection [23,24,43–46] of plasma electrons. Note that, although the bubble is fully formed for $x < L_1 + L_2$, no self-injection occurs prior to or after the laser's encountering

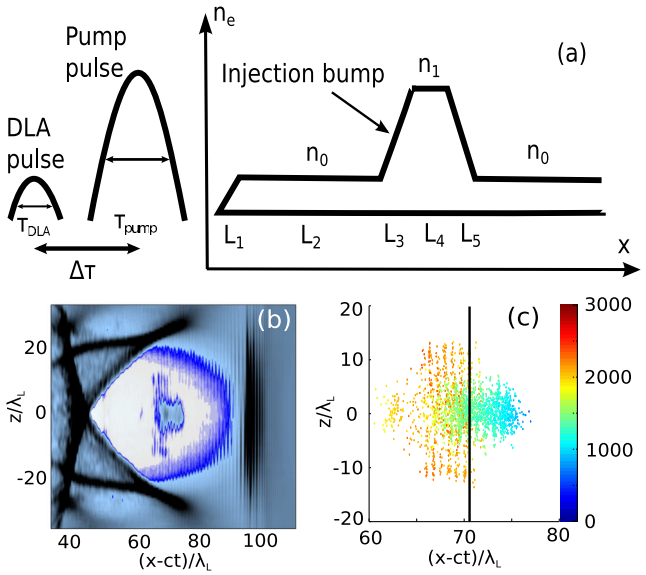


FIG. 3 (color online). (a) Schematic representation of the laser pulse format and plasma density profile. (b) Plasma electron density in the bubble regime at $x = 1$ cm; self-injected electron bunch has advanced approximately to the middle of the bubble. (c) Zoom in of the self-injected electrons color coded according to their relativistic factor $\gamma$. Black vertical line: bubble's center. Plasma parameters: $L_1 = L_3 = L_4 = L_5 = 0.1$ mm, $L_2 = 1.6$ mm; $n_0 = 1.8 \times 10^{18}$ cm$^{-3}$, $n_1 = 3n_0$, $\lambda_p \equiv 2\pi c/\omega_p = 26$ $\mu$m. Laser parameters: wavelengths $\lambda_L = 0.8$ $\mu$m, intensities $I_{\rm pump} = 2 \times 10^{19}$ W/cm$^2$ and $I_{\rm DLA} = I_{\rm pump}/5$, pulse durations $\tau_{\rm pump} = 50$ fs and $\tau_{\rm DLA} = 30$ fs, interpulse time delay $\Delta\tau = 67$ fs, spot sizes $w_L = 20$ $\mu$m. Simulation parameters: numerical grid's cell size $\Delta x \times \Delta z = \lambda_L/50 \times \lambda_p/50$, moving window size $W_x \times W_z = 120 \times 166.4$ $\mu$m, four macroparticles per cell.

the density bump. Experimental approaches to generating such density bumps have been described elsewhere [47,48]. The bump-facilitated injection can be thought of as a less "gentle" version of transverse injection [46] that imparts self-injected electrons with large transverse energy $\epsilon_\perp$ needed for efficient DLA as illustrated in Fig. 2(a).

As the injected electrons, shown in Fig. 3(b) after propagating for $x = 1$ cm through the plasma, advance towards the center of the bubble and experience dephasing, a clear separation into DLA and non-DLA groups occurs. Electrons color coded according to their final energy are shown in Fig. 3(c), which is a zoom in of Fig. 3(b) in the vicinity of the bubble's center indicated by a vertical black line. Clearly, the highest energy electrons comprising the DLA group have a much larger betatron oscillation amplitude, and are spatially located behind the lower-energy non-DLA group of electrons. According to Eq. (2), DLA electrons advance slower through the bubble because they have much higher transverse momentum (up to $p_z = 100 m_e c$) imparted directly by the DLA pulse.

The bifurcated $(x - ct, \gamma)$ phase space and the total energy spectrum of the accelerated electrons are plotted in Figs. 4(a) and 4(b), respectively (blue colored). The DLA (black circled) and non-DLA (red circled) electrons are clearly separated in energy and space, with their energy spectra peaking at $\epsilon_{\text{tot}}^{\text{DLA}} = 1.1$ GeV and $\epsilon_{\text{tot}}^{\text{n-DLA}} = 0.65$ GeV, respectively. To illustrate the role of the time-delayed DLA laser pulse on phase space bifurcation, we carried out PIC simulations for the single-pulse LWFA case, i.e., with the same bubble-producing pump pulse ($I_{\text{pump}} = 2 \times 10^{19}$ W/cm$^2$ corresponding to $a_{\text{pump}} = 3$) but no DLA pulse. The resulting electron phase space shown in Fig. 4(a) (black dots) does not show any phase space fragmentation, thus indicating that no DLA electrons are produced. We note in passing that the energy gain in the single-pulse case is somewhat smaller than for non-DLA particles in the two-pulse case because of the slightly weaker accelerating wake in the former case, apparently due to stronger on-axis beam loading.

The synergistic nature of the DLA and LWFA mechanisms can be demonstrated by comparing the LWFA gains $A_W$ plotted in Fig. 4(c) for two representative DLA and non-DLA electrons. Because it is impossible to rigorously separate laser and wake fields in PIC simulations, the energy gains $A_L$ and $A_W$ from the laser and wake were estimated [5] as $A_L = -\int eE_z v_z dt$ and $A_W = -\int eE_x v_x dt$, respectively, where $E_{x,z}$ is the electric field extracted from the PIC simulations. Even though the finite $E_x$ component of the laser pulse makes a nonvanishing contribution to $A_W$ for the off-axis electrons, we estimate that this contribution is much smaller than the contribution of the plasma wake.

From Fig. 4(c) we observe that the non-DLA electron gains less energy than the DLA electron, and promptly moves into the decelerating phase of the bubble's field (red solid line). The DLA electron does not experience

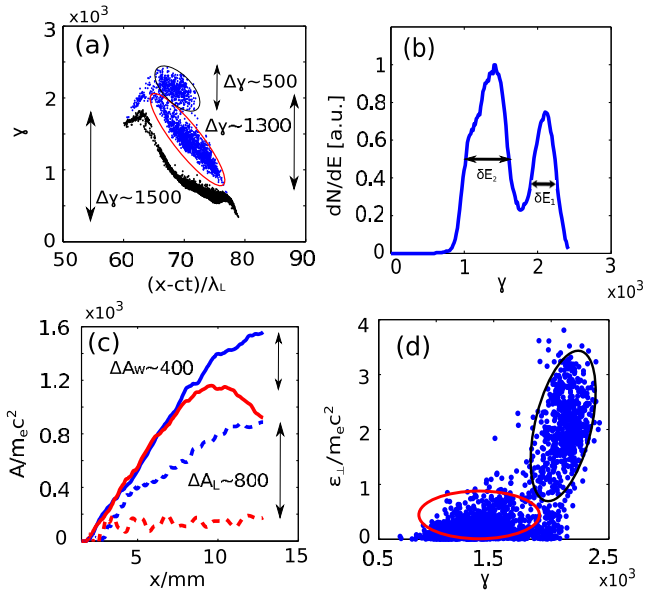


FIG. 4 (color online). (a) Phase space of self-injected electrons for double-pulse (blue dots) and single-pulse (black dots) laser formats. (b) Energy spectrum for double-pulse (pump + DLA) formats. Energy spreads: $\delta E_1 \simeq 350 m_e c^2$, $\delta E_2 \simeq 600 m_e c^2$. (c) Energy gain from the wake ($A_W$, solid lines) and laser ($A_L$, dashed line) fields for DLA (blue) and non-DLA (red) representative electrons. (d) Bifurcated phase space $(\gamma, \epsilon_\perp)$ shows correlation between total and transverse energies for DLA electrons.

dephasing (blue solid line), resulting in a much larger wake energy gain $A_W$. Additionally, the DLA electron gains considerable energy ($A_L \approx 900 m_e c^2$) directly from the laser. The combination of larger gains from the wake ($\Delta A_W \approx 400 m_e c^2$) and from the laser ($\Delta A_L \approx 800 m_e c^2$) explains why DLA electrons acquire much higher total energy $\gamma m_e c^2$ than non-DLA electrons [see Fig. 4(c) for definitions of $\Delta A_W$ and $\Delta A_L$]. A very strong positive correlation between $\gamma$ and $\epsilon_\perp$ within the DLA group of electrons is observed by plotting the $(\gamma, \epsilon_\perp)$ phase space in Fig. 4(d). No such correlation is observed for the non-DLA group.

In conclusion, we have proposed and theoretically demonstrated a new type of a plasma-based accelerator: a hybrid laser-wakefield and direct-laser accelerator. The synergistic nature of the LWFA and DLA mechanisms manifests itself in compounding the distinct energy gains from the plasma wake and directly from the laser pulse while increasing the former because of the delayed dephasing caused by the latter. Phase space bifurcation of the self-injected electrons into two distinct groups of high-energy DLA and lower-energy non-DLA particles is demonstrated. Future work will explore the possibility of developing incoherent and coherent radiation sources based on DLA electrons.

This work was supported by U.S. DOE Grants No. DE-SC0007889 and No. DE-SC0010622, and by AFOSR Grant No. FA9550-14-1-0045. The authors thank the Texas Advanced Computing Center (TACC) at The University of Texas at Austin for providing HPC resources.

[1] G. Mourou, B. Blocklesby, T. Tajima, and J. Limpert, Nat. Photonics **7**, 258 (2013).
[2] Y. Liu, X. J. Wang, D. B. Cline, M. Babzien, J. M. Fang, J. Gallardo, K. Kusche, I. Pogorelsky, J. Skaritka, and A. van Steenbergen, Phys. Rev. Lett. **80**, 4418 (1998).
[3] A. van Steenbergen, J. Gallardo, J. Sandweiss, and J.-M. Fang, Phys. Rev. Lett. **77**, 2690 (1996).
[4] A. Pukhov, Z.-M. Sheng, and J. Meyer-ter-Vehn, Phys. Plasmas **6**, 2847 (1999).
[5] C. Gahn, G. D. Tsakiris, A. Pukhov, J. Meyer-ter-Vehn, G. Pretzler, P. Thirolf, D. Habs, and K. J. Witte, Phys. Rev. Lett. **83**, 4772 (1999).
[6] D. H. Whittum, A. M. Sessler, and J. M. Dawson, Phys. Rev. Lett. **64**, 2511 (1990).
[7] T. Tajima and J. M. Dawson, Phys. Rev. Lett. **43**, 267 (1979).
[8] V. Malka, J. Faure, Y. A. Gauduel, E. Lefebvre, A. Rousse, and K. T. Phuoc, Nat. Phys. **4**, 447 (2008).
[9] E. Esarey, C. B. Schroeder, and W. P. Leemans, Rev. Mod. Phys. **81**, 1229 (2009).
[10] S. M. Hooker, Nat. Photonics **7**, 775 (2013).
[11] J. B. Rosenzweig, B. Breizman, T. Katsouleas, and J. J. Su, Phys. Rev. A **44**, R6189 (1991).
[12] A. Pukhov and J. Meyer-Ter-Vehn, Appl. Phys. B **74**, 355 (2002).
[13] J. Faure, Y. Glinec, A. Pukhov, S. Kiselev, S. Gordienko, E. Lefebvre, J. Rousseau, F. Burgy, and V. Malka, Nature (London) **431**, 541 (2004).
[14] C. Geddes, C. Toth, J. Van Tilborg, E. Esarey, C. Schroeder, D. Bruhwiler, C. Nieter, J. Cary, and W. Leemans, Nature (London) **431**, 538 (2004).
[15] S. Mangles, C. Murphy, Z. Najmudin, A. Thomas, J. Collier, A. Dangor, E. Divall, P. Foster, J. Gallacher, C. Hooker *et al.*, Nature (London) **431**, 535 (2004).
[16] W. Leemans, B. Nagler, A. Gonsalves, C. Toth, K. Nakamura, C. Geddes, E. Esarey, C. Schroeder, and S. Hooker, Nat. Phys. **2**, 696 (2006).
[17] X. Wang *et al.*, Nat. Commun. **4**, 1988 (2013).
[18] H. T. Kim, K. H. Pae, H. J. Cha, I. J. Kim, T. J. Yu, J. H. Sung, S. K. Lee, T. M. Jeong, and J. Lee, Phys. Rev. Lett. **111**, 165002 (2013).
[19] C. G. R. Geddes, K. Nakamura, G. R. Plateau, Cs. Toth, E. Cormier-Michel, E. Esarey, C. B. Schroeder, J. R. Cary, and W. P. Leemans, Phys. Rev. Lett. **100**, 215004 (2008).
[20] K. Schmid, A. Buck, C. M. S. Sears, J. M. Mikhailova, R. Tautz, D. Herrmann, M. Geissler, F. Krausz, and L. Veisz, Phys. Rev. ST Accel. Beams **13**, 091301 (2010).
[21] A. Buck, J. Wenz, J. Xu, K. Khrennikov, K. Schmid, M. Heigoldt, J. M. Mikhailova, M. Geissler, B. Shen, F. Krausz, S. Karsch, and L. Veisz, Phys. Rev. Lett. **110**, 185006 (2013).
[22] A. J. Gonsalves, K. Nakamura, C. Lin, D. Panasenko1, S. Shiraishi, T. Sokollik, C. Benedetti, C. B. Schroeder, C. G. R. Geddes, J. Van Tilborg *et al.*, Nat. Phys. **7**, 862 (2011).
[23] S. A. Yi, V. Khudik, C. Siemon, and G. Shvets, Phys. Plasmas **20**, 013108 (2013).
[24] S. Kalmykov, S. A. Yi, V. Khudik, and G. Shvets, Phys. Rev. Lett. **103**, 135004 (2009).
[25] F. S. Tsung, R. Narang, W. B. Mori, C. Joshi, R. A. Fonseca, and L. O. Silva, Phys. Rev. Lett. **93**, 185002 (2004).
[26] M. Tzoufras, W. Lu, F. S. Tsung, C. Huang, W. B. Mori, T. Katsouleas, J. Vieira, R. A. Fonseca, and L. O. Silva, Phys. Rev. Lett. **101**, 145002 (2008).
[27] K. Nemeth, B. Shen, Y. Li, H. Shang, R. Crowell, K. C. Harkay, and J. R. Cary, Phys. Rev. Lett. **100**, 095002 (2008).
[28] I. Nam, M. S. Hur, H. S. Uhm, N. A. M. Hafz, and H. Suk, Phys. Plasmas **18**, 043107 (2011).
[29] J. L. Shaw, F. S. Tsung, N. Vafaei-Najafabadi, K. A. Marsh, N. Lemos, W. B. Mori, and C. Joshi, Plasma Phys. Controlled Fusion **56**, 084006 (2014)
[30] A. P. L. Robinson, A. V. Arefiev, and D. Neely, Phys. Rev. Lett. **111**, 065002 (2013).
[31] A. V. Arefiev, V. N. Khudik, and M. Schollmeier, Phys. Plasmas **21**, 033104 (2014).
[32] S. Cipiccia, M. R. Islam, B. Ersfeld, R. P. Shanks, E. Brunetti, G. Vieux, X. Yang, R. C. Issac, S. M. Wiggins, G. H. Welsh *et al.*, Nat. Phys. **7**, 867 (2011).
[33] K. Ta. Phuoc, S. Corde, R. Fitour, R. Shah, F. Albert, J-P Rousseau, F. Burgy, A. Rousse, V. Seredov, and A. Pukhov, Phys. Plasmas **15**, 073106 (2008).
[34] K. Ta Phuoc, E. Esarey, V. Leurent, E. Cormier-Michel, C. G. R. Geddes, C. B. Schroeder, A. Rousse, and W. P. Leemans, Phys. Plasmas **15**, 063102 (2008).
[35] T. Tajima, Y. Kishimoto, and M. C. Downer, Phys. Plasmas **6**, 3759 (1999).
[36] P. Serafim, P. Sprangle, and B. Hafizi, IEEE Trans. Plasma Sci. **28**, 1155 (2000).
[37] A. G. York, H. M Milchberg, J. P. Palastro, and T. M. Antonsen, Phys. Rev. Lett. **100**, 195001 (2008).
[38] I. Kostyukov, A. Pukhov, and S. Kiselev, Phys. Plasmas **11**, 5256 (2004).
[39] S. Corde, K. T. Phuoc, R. Fitour, J. Faure, A. Tafzi, J. P. Goddet, V. Malka, and A. Rousse, Phys. Rev. Lett. **107**, 255003 (2011).
[40] H. Guo, L. Chen, H. Keren, J. L. Hirshfield, S. Y. Park, and K. R. Chu, Phys. Rev. Lett. **49**, 730 (1982).
[41] M. Einat and E. Jerby, Phys. Rev. E **56**, 5996 (1997).
[42] A. Pukhov, J. Plasma Phys. **61**, 425 (1999).
[43] S. A. Yi, V. Khudik, S. Y. Kalmykov, and G. Shvets, Plasma Phys. Controlled Fusion **53**, 014012 (2011).
[44] A. Pak, K. A. Marsh, S. F. Martins, W. Lu, W. B. Mori, and C. Joshi, Phys. Rev. Lett. **104**, 025003 (2010).
[45] H. Suk, N. Barov, J. B. Rosenzweig, and E. Esarey, Phys. Rev. Lett. **86**, 1011 (2001).
[46] R. Lehe, A. F. Lifschitz, X. Davoine, C. Thaury, and V. Malka, Phys. Rev. Lett. **111**, 085005 (2013).
[47] C.-H. Pai, S.-Y. Huang, C.-C. Kuo, M.-W. Lin, J. Wang, S.-Y. Chen, C.-H. Lee, and J.-Y. Lin, Phys. Plasmas **12**, 070707 (2005).
[48] M.-W. Lin, Y.-M. Chen, C.-H. Pai, C.-C. Kuo, K.-H. Lee, J. Wang, S.-Y. Chen, and J.-Y. Lin, Phys. Plasmas **13**, 110701 (2006).